

Control Algorithm Technique for Multilevel Cascaded H-Bridge Inverters

Davu.srinivasa rao

Assistant professor
Department of Electrical & Electronics Engineering
Mallareddy institute of engineering and technology
Sri.davu@gmail.com

Davu.Dhanunjaya

Research & Development in GE Energy
Chennai
davu.1212@gmail.com

Abstract:

Multi cell converters are one of the alternative topologies for medium-voltage industrial drives. For an application requiring regenerative capability, each power cell must be constructed with a three- or single-phase pulse width-modulation (PWM) rectifier as front end. Multi level cascaded H-bridge (CHB) converters have been presented as a good solution for high-power applications. The choice of single-phase PWM rectifiers for the input of the cells results in a reduced number of power switches and a simpler input transformer than the three phase equivalent. However, its control is not as straightforward. In this paper, the steady-state power balance in the cells of a single-phase two-cell CHB is studied. The ability to receive active power network or to deliver active power to the grid in each cell is analyzed according to the DC-link voltage and the desired output AC voltage value. Simulation results are shown to validate the presented analysis.

I.INTRODUCTION

MULTILEVEL inverters can provide an efficient alternative to high power applications, providing a high quality output voltage, increasing the efficiency and robustness, and reducing the electromagnetic interference. There are three well established topologies of multilevel inverters: neutral point clamped (NPC) [1], flying capacitor [2], and cascaded H-bridge (CHB) [3], [4]. This paper deals with the CHB inverter topology which is based on a series connection of many single-phase H-bridge inverters to provide the total output voltage required by the load [5], [6]. The CHB inverter with equal dc sources has a large number of redundant switching combinations that synthesize the same output voltage per phase [7]. Using asymmetrical dc sources, it is possible to reduce the redundancies, increasing the output voltage levels [8]. Therefore, a high quality output voltage can be achieved using only a few H-bridge inverters [9], featuring a very low harmonic content, reduced common mode voltage [10] and practically no electromagnetic compatibility issues [11]. Considering the high quality output voltage provided by

this converter, applications like high power drives [12], [13] and Static Compensators (STATCOMs) [14] have been proposed. The modularity provided by the CHB is very attractive for STATCOM applications, because the dc sources can be replaced by capacitors which provide the reactive power required to compensate the load current [15]. Predictive control relies on a model of the inverter and basically calculates the error of a cost function for each possible input, selecting the input that minimizes this function. Predictive control algorithms exhibit a high dynamic and a very good performance when applied to power electronics [16]; this feature can be achieved because the power electronics devices, in spite of its nonlinear characteristic, can be modeled accurately [17], and using a parameter estimation scheme, the model uncertainties can be adjusted [18]. In addition, the inputs belong to a finite set of switching combinations [19], reducing the processing time used to perform the optimization. Predictive control has been successfully applied to two-level three-phase inverters [20], where the cost function is related to minimize the error of the output current and a given current reference. Cost functions with higher complexity can be implemented, incorporating the model of the load to provide a direct power control [21], [22], the model of an induction motor to provide flux and torque control capability [23], or impose a desired load current spectrum [24]. Multilevel inverters have a higher number of switching combinations than a two-level inverter [25]. Hence, the number of iterations to implement the predictive algorithm, as well as the processing time, is greatly increased. This requirement degrades the overall performance, and the implementation of predictive control could become impracticable when the sample time is large enough. However, the predictive control of three level NPC inverters has been reported [26]. The NPC inverter has the property that does not have switching redundancy, i.e., each possible output voltage has one and only one switching combination; therefore, the processing time could remain small. In [27], an extension of the algorithm is proposed and tested in a four-level NPC. It is possible to reduce the processing



time required by predictive control, using the fact that the solution of the discrete model can be expressed directly in terms of the state variables. Therefore, this function does not have to be evaluated in each optimization iteration.

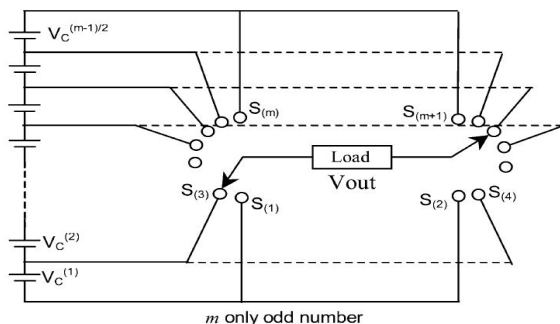


Figure1: The m-level inverter using an “H” bridge

II. CASCADED MULTILEVEL INVERTER

Another characteristic is that the “H” topology has many redundant combinations of switches’ positions to produce the same voltage levels. As an example, the level “zero” can be generated with switches in position S(1) and S(2), or S(3) and S(4), or S(5) and S(6), and so on. Another characteristic of “H” converters is that they only produce an odd number of levels, which ensures the existence of the “0V” level at the load as shown in figure 1 .For example, a 51-level inverter using an “H” configuration with transistor-clamped topology requires 52 transistors, but only 25 power supplies instead of the 50 required when using a single leg. Therefore, the problem related to increasing the number of levels and reducing the size and complexity has been partially solved, since power supplies have been reduced to 50% as shown in figure 2.

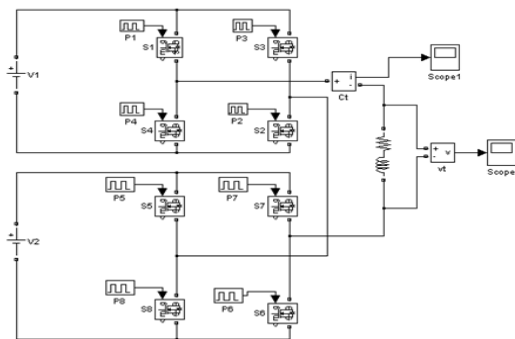


Figure2: Multilevel Cascaded H-Bridge Converter

III. MODULATION TECHNIQUES FOR CHB CONVERTERS

Different multilevel modulation techniques for CHB converters have been presented in the literature. Many of these techniques have been extended from classic pulse width modulation (PWM) and SVM methods. Level-shifted and phase shifted PWMs are derived from classic PWM methods that use triangular carriers , it is reported that the phase-shifted PWM modulation is the natural method for CHB converters achieving good-quality output voltage with a fundamental component that is *N* times the fundamental component of each cell for an *N*-cell CHB converter. Multilevel SVM techniques have been presented and achieve simplicity, offering an alternative to carrier-based PWM techniques [28]–[32]. SVM strategies are based on the generation of the reference voltage that was determined by the controller as the average of the discrete output voltages that can be achieved by the power converter. These techniques take advantage of the degrees of freedom as the selection of the switching sequence can be made in order to improve some power converter feature, such as the number of commutations or voltage balance [33], [34] as shown in figure 2. However, both the PWM and SVM methods have problems when the multilevel converter is operated with uncontrolled dc-link voltages. With CHB converters, if the dc voltages are not of the correct magnitude and the modulators do not take these voltage errors into account, there will be distortion in the output waveforms.

A). SYSTEM DESCRIPTION

A single-phase 2C-CHB power converter is shown in Fig. 2.The system is connected to the grid through a smoothing inductor *L*. Load behavior is considered by using current sources *iL1* and *iL2* connected to each dc-link capacitor *C1* and *C2*, respectively. The equations that describe the 2C-CHB behavior are well known, and they have been reported previously [35]

$$\begin{aligned}
 v_{m1} &= \delta_1 v_{dc1} & p_1 &= v_{dc1} i_{L1} \\
 v_{m2} &= \delta_2 v_{dc2} & p_2 &= v_{dc2} i_{L2} \\
 p_t &= p_1 + p_2 & & \dots \dots \dots (1)
 \end{aligned}$$

$$V_s = L \frac{dI_s}{dt} + v_{m1} + v_{m2} \dots \dots \dots (2)$$

$$v_{m1} I_s = C_1 \frac{d}{dt} \left(\frac{v_{dc1}^2}{2} \right) + p_1 \dots \dots \dots (3)$$

$$v_{m2} I_s = C_2 \frac{d}{dt} \left(\frac{v_{dc2}^2}{2} \right) + p_2 \dots \dots \dots (4)$$

The behavior of 2C-CHB is characterized by the inductor current dynamic (2) and dc-link capacitor voltage dynamic in each cell (3) and (4). In these equations, signals $vm1$ and $vm2$ represent the output voltages of each cell. These voltages depend on the dc-link voltage and the control signal values in each cell. Moreover, signals $p1$ and $p2$ are the instantaneous powers demanded or delivered by the current sources connected to each cell, respectively. To analyze the steady-state power balance in the cells of a cascaded converter. In this representation, the cells have been replaced by voltage sources with values $v1$ and $v2$ that are equal to the rms values of the fundamental harmonic of the voltages modulated by the cells $vm1,1$ and $vm2,1$, respectively. Output phase voltage (vab), grid voltage (vs), and grid current (is) are considered in the equivalent circuit

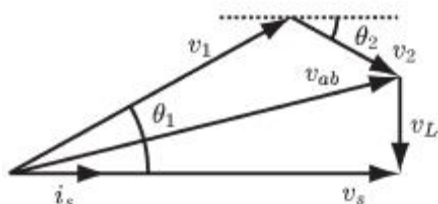


Figure 3. 2C-CHB Phasorial digram of the voltages and currents

$$X_y = \sqrt{\frac{1}{T} \int_0^T X_{y,1}^2 dt} \dots\dots\dots (5)$$

The rms values can be calculated from the fundamental harmonic value of each variable using (5), where xy represents the rms and $Xy,1$ represents the fundamental harmonics

$$P_y = v_y i_y \cos \theta_y \dots\dots\dots (6)$$

$$Q_y = v_y i_y \sin \theta_y \dots\dots\dots (7)$$

The equivalent circuit is composed by sinusoidal voltage sources and passive components. As a consequence, it is possible to analyze it using conventional active and reactive power definitions under sinusoidal conditions for single-phase systems [36]. In (6) and (7), v_y and i_y are the rms values of the voltage and current, respectively, and θ_y represents the shift angle between them. Moreover, P_y is the active power which is equal to the mean value of the instantaneous power p_y , and Q_y is the reactive power.

IV. SIMULATION RESULTS

In this section, simulation results are shown to validate the analysis presented in Section III. For this purpose, a single phase 2C-CHB converter prototype has been used.

A. Stable Operation With $vc1 \leq vab$ and $vc2 \leq vab$

In this case, it is necessary to use both cells to generate the output voltage vab . Fig. 4 shows in a red marked area the possible points to achieve the desired output voltage. Any point outside of this region makes the system unstable because the output voltage cannot be modulated with those values of the dc-link capacitor voltages. In addition, as shown in the figure, the projection of v_1 over i_s is always positive, and the same occurs for v_2 ; as a consequence, the active power values in both cells are positive, meaning that the grid supplies active power to both cells simultaneously. Moreover, it is not possible to find a point where the grid supplies active power to one cell and, at the same time, the other cell delivers active power to the grid.

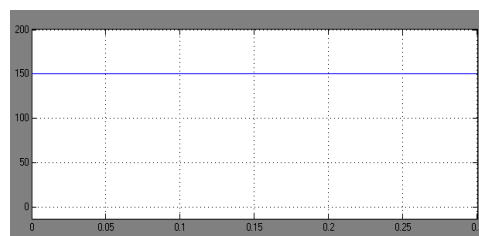


Figure 4: Inverter-1 input voltage

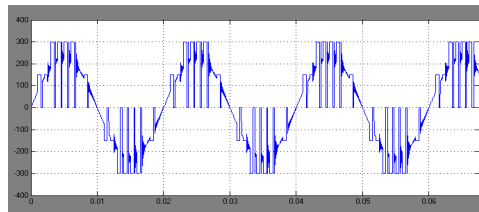


Figure 5: Multi level Inverter output voltage

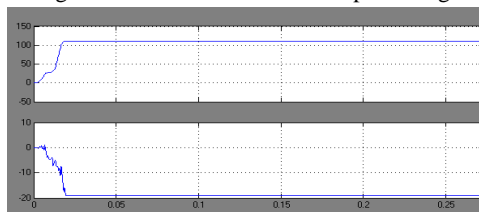


Figure 6: Real and reactive power

In addition, this situation means that it is not possible to have the grid supplying active power only to one cell or to have only one cell delivering active power to the grid. On the other hand, it can be observed that the reactive power exchanged with the inductor is supplied by the cells. There is no restriction to the reactive power sign contributed by each cell. This means that the

reactive power in each cell can be different; even in one cell; the reactive power can have a capacitive nature while the other has an inductive nature. In Fig. 5, it is shown that, for a given total amount of active power supplied by the grid to the converter, the power delivered to each cell has to be between a minimum and a maximum value to achieve a stable operation. Fig. 5 shows the minimum active power that has to be supplied to cell 1. This value corresponds with the minimum reachable length of the projection of v_1 over is , represented in the figure with $v_{\min} 1p$. As the total amount of active power is fixed, this value is related with the maximum active power that can be delivered to cell 2. It can be noticed that the dc output voltage references are achieved without difficulties. Moreover, I_s grows or decreases in accordance with the output load value variations. In addition, the input current is almost in phase with the input voltage and presents a low total harmonic distortion (THD), This input current has a PF of 0.99 and a THD of 2.5%. This THD value has been calculated up to the 50th harmonic order.

B. Unstable Operation With $vc_1 \leq v_{ab}$ and $vc_2 \leq v_{ab}$

In this case, the desired output voltage can be achieved using both cells or just using the cell with the higher dc voltage. This allows two possible power balance situations in the cells. In Fig. 6, the marked red area represents the points where both cells are supplied with active power from the grid, while the marked green area shows the points where the first cell is supplied with active power from the grid while the second cell delivers active power to the grid. As in Section III-A, the reactive power is exchanged between the inductor and the cells without restrictions in the reactive power sign contributed by each one. Fig. 7 shows a possible solution with both cells supplied with active power from the grid, and Fig. 8 shows a possible solution when the first cell is supplied from the grid while the second cell delivers active power to the grid. It is worth noting that, when $vc_1 > v_{ab}$ and $vc_2 \leq v_{ab}$, if the total active power supplied to the converter from the grid is positive, then only the second cell active power can be negative, while the first cell active power is positive; it is not possible to have a negative active power in the first cell while the second cell has a positive active power value. Fig.8 shows the limits for the maximum and minimum active power values allowed in the cells to achieve a stable operation, when the total amount of active power supplied from the grid to the converter is fixed. Two different power balance situations can be clearly identified.

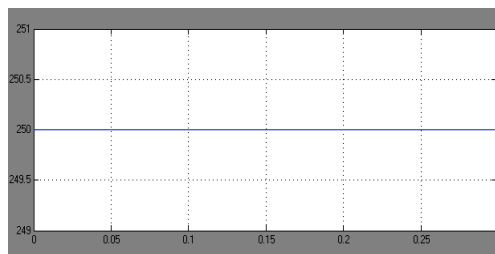


Figure 7: Inverter-1 input voltage

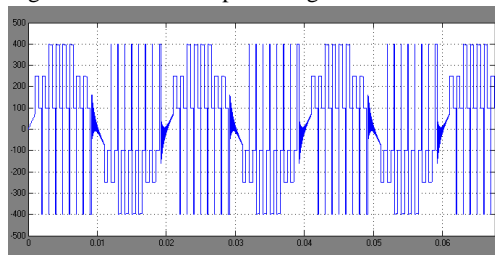


Figure 8: Multi level Inverter output voltage

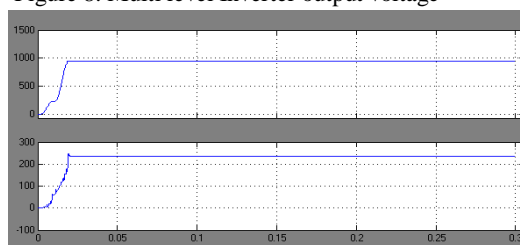


Figure 9: Real and reactive power

The first one can be considered as the conventional operation of the converter. In this case, both cells are supplied from the grid, and as a consequence, a minimum active power has to be supplied to cell 1 from the grid; this value corresponds with the minimum reachable length of the projection of v_1 over is , represented in the figure with $v_{\min} 1p$. Associated with this value is $v_{\max} 2p$, which is the maximum reachable length of the projection of v_2 over is and represents the maximum active power that can be supplied to cell 2.

The second power balance situation, shown in Fig. 13, implies that the active powers in each cell have different signs. Thus, the cell with the higher dc voltage is supplied from the grid, while the other cell is delivering active power to the grid. Under this situation, the values for the maximum active power that can be delivered to cell 1 $v_{\max} 1p$ and the minimum active power that has to be supplied to cell 2 $v_{\min} 2p$ can be defined. In Fig. 14, it can be noticed that $v_{\min} 2p$ has opposite direction than is ; thus, the second cell is delivering active power. Moreover, the maximum active power supplied to cell 1 is higher than the total amount of active powers delivered from the grid. Initially, the converter is operated with a load located inside the stable region. For this purpose, two resistors of 40Ω are connected to the cells, consuming 1 kW in each cell. Then, a load step is

applied to the converter in such a way that the converter goes to an unstable point. To achieve this condition, a resistor of 100 Ω is connected in the first cell and 25 Ω to the second cell, drawing 1.6 and 0.4 kW, respectively

$$P_1^{\max} = \frac{V_{1p}^{\max}}{V_s} P_t \dots\dots\dots (8)$$

$$P_1^{\min} = \frac{(V_s - V_{2p}^{\max})}{V_s} P_t \dots\dots\dots (9)$$

$$P_2^{\max} = \frac{V_{2p}^{\max}}{V_s} P_t \dots\dots\dots (10)$$

$$P_2^{\min} = \frac{(V_s - V_{1p}^{\max})}{V_s} P_t \dots\dots\dots (11)$$

From the figure 13 and 14 It can be noticed that, for the first load configuration, the converter achieves a stable operation, the dc voltages are stable in the reference commands, and the input current is established in agreement with the output load. When the load step is applied, the converter tries to follow the references; however, as it is working outside the stable region, it is not possible to achieve the commands and the dc voltages change without control. Finally, the converter has to be stopped to avoid a malfunction caused by the input current or by a high output voltage value.

C. Stable Operation with $vc1 > vab$ and $vc2 \leq vab$

In this case, the output voltage can be modulated using both cells or just using one of them. As a consequence, three possible power balance situations in the cells are under concern. In the marked red area of Fig. 10, both cells are supplied simultaneously with active power from the grid, whereas the marked green area shows the set of points where the first cell is supplied with active power from the grid while the second cell delivers active power to the grid. On the other hand, the marked light blue area represents the set of points where the first cell delivers active power to the grid while the second cell is supplied with active power from the grid. Again, the reactive power is exchanged between the smoothing inductor and the cells without restrictions in the sign of the reactive power of each cell.

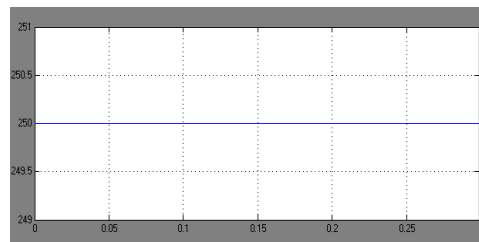


Figure 10: Inverter-1 input voltage

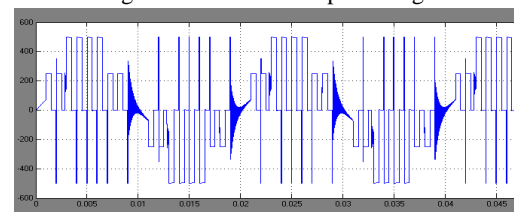


Figure 11: Multi level Inverter output voltage

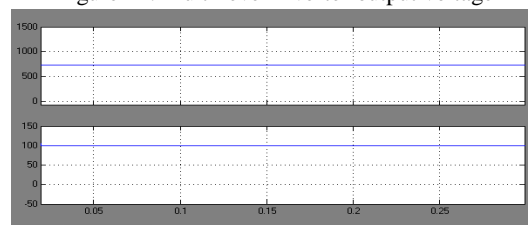


Figure 12: Real and reactive power

Fig. 10 shows the three possible solutions, one for each power balance situation under concern. Fig. 11 shows the conventional operation, where both cells are supplied with active power from the grid. Fig. 12 shows the converter operation when the first cell is supplied from the grid while the second cell delivers active power to the grid. Finally, it shows a solution with the first cell delivering active power to the grid while the second cell is supplied with active power from the grid. It can be noticed that, when $vc1 > vab$ and $vc2 > vab$, although the total active power supplied to the converter from the grid is positive, it is possible that any one cell delivers active power to the grid while the other one is supplied with active power from the grid. When the maximum and minimum limits of the active power consumed or injected by the loads connected to the cells are analyzed, when the power balance through each cell has different signs, are found, the maximum active power that can be supplied and the minimum active power values that have to be delivered to each cell to achieve a stable operation, for a given total amount of active powers consumed by the loads connected to the converter, are shown.

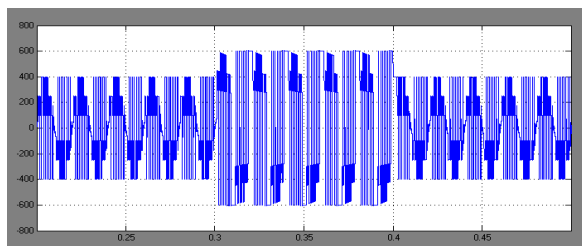


Figure 13: Multilevel inverter fed grid system with output variations of current through grid

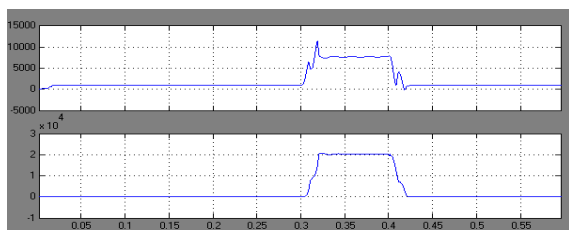


Figure 14: Multilevel inverter fed grid system with output variations of real and reactive power

To develop the test, the following steps are applied. In the beginning, both cells are controlled to 200 V, and a resistor of 100 Ω is connected to each cell. When steady state is achieved, the first cell command is changed to 400 V; thus, the converter load is consuming 2 kW with both cells supplied with active power from the grid. Then, after 1 s, a current source is connected to the second cell to supply power from the cell to the grid. For this purpose, the source injects a current of 1.7 A so that the final active power value supplied to the converter from the grid is 1.7 kW, but the first cell is supplied from the grid while the second cell delivers active power to the grid. However, the controller evacuates this power, achieving the voltage reference commands. When grid current is observed (Fig. 18), it can be appreciated that the current amplitude decreases when the active power is supplied from the second cell; thus, there is an energy transfer from the second cell to the first cell.

V. CONCLUSION

A CHB power converter is a suitable topology to be used when two or more independent dc voltage values are needed in a synchronous rectifier or back-to-back application. However, some criteria have to be taken into account to achieve a stable converter operation. In this paper, the power balance limits in the cells of a single-phase 2C-CHB power converter have been addressed. These limits depend on the dc-link voltage values. It is shown that, under certain conditions, it is possible to have opposite sign active power values simultaneously in both cells. Moreover, to have a stable operation, it is necessary to ensure that, for a total amount of active power supplied to the 2C-CHB, both cell loads are

between the maximum and minimum allowed. Finally, simulation results are introduced, validating that the presented analysis is an appropriate tool to establish the design criteria for the 2C-CHB synchronous rectifier or back-to-back application.

REFERENCES

- [1] J. Rodriguez, S. Bernet, B. Wu, J. Pontt, and S. Kouro, "Multilevel voltage-source-converter topologies for industrial medium-voltage drives," *IEEE Trans. Ind. Electron.*, vol. 54, no. 6, pp. 2930–2945, Dec. 2007.
- [2] L. Xu and V. G. Agelidis, "VSC transmission system using flying capacitor multilevel converters and hybrid PWM control," *IEEE Trans. Power Del.*, vol. 22, no. 1, pp. 693–702, Jan. 2007.
- [3] M. A. Perez, J. R. Espinoza, J. Rodriguez, and P. Lezana, "Regenerative medium-voltage ac drive based on a multicell arrangement with reduced energy storage requirements," *IEEE Trans. Ind. Electron.*, vol. 52, no. 1, pp. 171–180, Feb. 2005.
- [4] P. Lezana, J. Rodriguez, and D. A. Oyarzun, "Cascaded multilevel inverter with regeneration capability and reduced number of switches," *IEEE Trans. Ind. Electron.*, vol. 55, no. 3, pp. 1059–1066, Mar. 2008.
- [5] C. R. Baier, J. I. Guzman, J. R. Espinoza, M. A. Perez, and J. R. Rodriguez, "Performance evaluation of a multi cell topology implemented with single-phase non regenerative cells under unbalanced supply voltages," *IEEE Trans. Ind. Electron.*, vol. 54, no. 6, pp. 2969–2978, Dec. 2007.
- [6] P. Lezana, C. A. Silva, J. Rodriguez, and M. A. Perez, "Zero-steady-state error input-current controller for regenerative multilevel converters based on single-phase cells," *IEEE Trans. Ind. Electron.*, vol. 54, no. 2, pp. 733–740, Apr. 2007.
- [7] R. Gupta, A. Ghosh, and A. Joshi, "Switching characterization of cascaded multilevel-inverter-controlled systems," *IEEE Trans. Ind. Electron.*, vol. 55, no. 3, pp. 1047–1058, Mar. 2008.
- [8] C. Rech and J. R. Pinheiro, "Hybrid multilevel converters: Unified analysis and design considerations," *IEEE Trans. Ind. Electron.*, vol. 54, no. 2, pp. 1092–1104, Apr. 2007.
- [9] Z. Du, L. M. Tolbert, J. N. Chiasson, and B. Ozpineci, "Reduced switching-frequency active harmonic elimination for multilevel converters," *IEEE Trans. Ind. Electron.*, vol. 55, no. 4, pp. 1761–1770, Apr. 2008.
- [10] C. Rech and J. R. Pinheiro, "Impact of hybrid multilevel modulation strategies on input and output harmonic performances," *IEEE Trans. Power Electron.*, vol. 22, no. 3, pp. 967–977, May 2007.

- [11] Y. Liu and F. L. Luo, "Trinary hybrid 81-level multilevel inverter for motor drive with zero common-mode voltage," *IEEE Trans. Ind. Electron.*, vol. 55, no. 3, pp. 1014–1021, Mar. 2008.
- [12] J. Dixon, A. A. Breton, F. E. Rios, J. Rodriguez, J. Pontt, and M. A. Perez, "High-power machine drive, using non redundant 27-level inverters and active front end rectifiers," *IEEE Trans. Power Electron.*, vol. 22, no. 6, pp. 2527–2533, Nov. 2007.
- [13] S. Kouro, R. Bernal, H. Miranda, C. A. Silva, and J. Rodriguez, "High performance torque and flux control for multilevel inverter fed induction motors," *IEEE Trans. Power Electron.*, vol. 22, no. 6, pp. 2116–2123, Nov. 2007.
- [14] J. D. L. Morales, M. F. Escalante, and M. Mata-Jimenez, "Observer for DC voltages in a cascaded H-bridge multilevel STATCOM," *IET Elect. Power Appl.*, vol. 1, no. 6, pp. 879–889, Nov. 2007.
- [15] Q. Song, W. Liu, and Z. Yuan, "Multilevel optimal modulation and dynamic control strategies for STATCOMs using cascaded multilevel inverters," *IEEE Trans. Power Del.*, vol. 22, no. 3, pp. 1937–1946, Jul. 2007.
- [16] P. Athalye, D. Maksimovic, and R. Erickson, "Variable-frequency predictive digital current mode control," *IEEE Power Electron. Lett.*, vol. 2, no. 4, p. 113–116, Dec. 2004.
- [17] P. Merceorelli, N. Kubasiak, and S. Liu, "Model predictive control of an electromagnetic actuator fed by multilevel PWM inverter," in *Proc. IEEE Int. Symp. Ind. Electron.*, May 4–7, 2004, vol. 1, pp. 531–535.
- [18] S.-J. Jeong and S.-H. Song, "Improvement of predictive current control performance using online parameter estimation in phase controlled rectifier," *IEEE Trans. Power Electron.*, vol. 22, no. 5, pp. 1820–1825, Sep. 2007.
- [19] J. Rodriguez, J. Pontt, C. Silva, M. Salgado, S. Rees, U. Ammann, P. Lezana, R. Huerta, and P. Cortes, "Predictive control of three-phase inverter," *Electron. Lett.*, vol. 40, no. 9, pp. 561–563, Apr. 29, 2004.
- [20] J. Rodriguez, J. Pontt, C. A. Silva, P. Correa, P. Lezana, P. Cortes, and U. Ammann, "Predictive current control of a voltage source inverter," *IEEE Trans. Ind. Electron.*, vol. 54, no. 1, pp. 495–503, Feb. 2007.
- [21] S. A. Larrinaga, M. A. R. Vidal, E. Oyarbide, and J. R. T. Apraiz, "Predictive control strategy for DC/AC converters based on direct power control," *IEEE Trans. Ind. Electron.*, vol. 54, no. 3, pp. 1261–1271, Jun. 2007.
- [22] J. Rodriguez, J. Pontt, P. Correa, P. Lezana, and P. Cortes, "Predictive power control of an AC/DC/AC converter," in *Conf. Rec. 14th IEEE IAS Annu. Meeting*, Oct. 2005, vol. 2, pp. 934–939.
- [23] J. Rodriguez, J. Pontt, C. Silva, P. Cortes, U. Ammann, and S. Rees, "Predictive current control of a voltage source inverter," in *Proc. 35th Annu. IEEE PESC*, Jun. 20–25, 2004, pp. 2192–2196.
- [24] P. Cortes, J. Rodriguez, D. E. Quevedo, and C. Silva, "Predictive current control strategy with imposed load current spectrum," *IEEE Trans. Power Electron.*, vol. 23, no. 2, pp. 612–618, Mar. 2008.
- [25] O. Lopez, J. Alvarez, J. Doval-Gandoy, and F. D. Freijedo, "Multilevel multiphase space vector PWM algorithm," *IEEE Trans. Ind. Electron.*, vol. 55, no. 5, pp. 1933–1942, May 2008.
- [26] R. Vargas, P. Cortes, U. Ammann, J. Rodriguez, and J. Pontt, "Predictive control of a three-phase neutral-point-clamped inverter," *IEEE Trans. Ind. Electron.*, vol. 54, no. 5, pp. 2697–2705, Oct. 2007.
- [27] G. S. Perantzakis, F. H. Xepapas, and S. N. Manias, "Efficient predictive current control technique for multilevel voltage source inverters," in *Proc. Eur. Conf. Power Electron. Appl.*, Sep. 11–14, 2005. CD-ROM.
- [28] A. K. Gupta and A. M. Khambadkone, "A space vector PWM scheme for multilevel inverters based on two-level space vector PWM," *IEEE Trans. Ind. Electron.*, vol. 53, no. 5, pp. 1631–1639, Oct. 2006.
- [29] M. M. Prats, J.M. Carrasco, and L. G. Franquelo, "Effective algorithm for multilevel converters with very low computational cost," *Electron. Lett.*, vol. 38, no. 22, pp. 1398–1400, Oct. 24, 2002.
- [30] N. Celanovic and D. Boroyevich, "A fast space-vector modulation algorithm for multilevel three-phase converters," *IEEE Trans. Ind. Appl.*, vol. 37, no. 2, pp. 637–641, Mar./Apr. 2001.
- [31] C. Rech and J. R. Pinheiro, "Hybrid multilevel converters: Unified analysis and design considerations," *IEEE Trans. Ind. Electron.*, vol. 54, no. 2, pp. 1092–1104, Apr. 2007.
- [32] O. Bouhali, E. M. Berkouk, B. Francois, and C. Saudemont, "Direct generalized modulation of electrical conversions including self stabilization of the dc-link for a single phase multilevel inverter based ac grid interface," in *Proc. IEEE PESC*, 2004, pp. 1385–1391.
- [33] J. Pou, R. Pindado, D. Boroyevich, P. Rodriguez, and J. Vicente, "Voltage balancing strategies for diode-clamped multilevel converters," in *Proc. IEEE PESC*, Jun. 20–25, 2004, vol. 5, pp. 3988–3993.

- [34] J. I. Leon, G. Guidi, L. G. Franquelo, T. Undeland, and S. Vazquez, “Simple control algorithm to balance the dc-link voltage in multilevel four-leg four-wire diode clamped converters,” in *Proc. 12th Int. EPE-PEMC*, Aug. 2006, pp. 228–233
- [35] A. Dell’Aquila, M. Liserre, V. G. Monopoli, and P. Rotondo, “An energy based control for an n-H-bridges multilevel active rectifier,” *IEEE Trans. Ind. Electron.*, vol. 52, no. 3, pp. 670–678, Jun. 2005.
- [35] IEEE Trial-Use Standard Definitions for the Measurement of Electric Power Quantities Under Sinusoidal, Non sinusoidal, Balanced, or Unbalanced Conditions, IEEE Std. 1459-2000, Jan. 2000.
- [36] H. Akagi, E. H. Watanabe, and M. Aredes, *Instantaneous Power Theory and Applications to Power Conditioning*, 1st ed. Hoboken, NJ: Wiley, 2007.